

Syntheses and crystal structures of mono- and bi-metallic zinc compounds of symmetrically- and asymmetrically-substituted bis(amino)cyclodiphosph(V)azanes

Graham R. Lief^a, Daniel F. Moser^a, Lothar Stahl^{a,*}, Richard J. Staples^b

^a Department of Chemistry, University of North Dakota, Box 9024, Grand Forks, ND 58202-9024, USA

^b Department of Chemistry and Chemical Biology, Harvard University, Cambridge, MA 02138, USA

Received 16 October 2003; accepted 5 January 2004

Abstract

The dioxocyclodiphosph(V)azane *cis*-[('BuHN)O=P(μ-N'Bu)₂P=O(NH'Bu)] reacted with two equivalents of diethylzinc to form the centrosymmetric dimer {[O=PN'Bu)₂(N'Bu)₂ZnEt(ZnEt·THF)]₂ (**1**) while under identical conditions, the sulfur and selenium analogues afforded only the monoethylzinc compounds {[('BuHN)E=P(μ-N'Bu)₂P=E(N'Bu)](ZnEt·THF)}E=S(**2**), Se (**3**). To further probe the apparent ligand effects on coordination number and coordination site, *cis*-[(PhHN)S=P(μ-N'Bu)₂P=S(NH'Bu)] (**5**) was synthesized from *cis*-[CIP(μ-N'Bu)₂P(NH'Bu)] (**4**) and both were characterized by single-crystal X-ray diffraction. Two equivalents of **5** reacted with diethylzinc to produce the homoleptic, trispirocyclic complex {[('BuHN)S=P(μ-N'Bu)₂P=S(NPh)]₂Zn} (**6**). A second asymmetrically-substituted cyclodiphosph(V)azane, namely [(('BuNH)S=P(μ-N'Bu)₂P=Np-tol(NH'Bu)] (**7**), was also synthesized and structurally characterized. In contrast to **5**, only one equivalent of this ligand reacted with excess diethylzinc, via its *N,N'*, rather than its *N,S* side, to afford {[('BuHN)S=P(μ-N'Bu)₂P=Np-tolyl(N'Bu)](ZnEt)} (**8**). © 2004 Elsevier B.V. All rights reserved.

Keywords: Zinc; Ethylzinc-amides; Ambidentate ligands; Cyclodiphosph(V)azanes; Diazadiphosphetidines

1. Introduction

Ambidentate inorganic ligands, e.g., NO₂⁻ and SCN⁻, have played an important role in the development of coordination chemistry, because they have provided important insight into electronic metal–ligand interactions [1,2]. As the structural complexity of ligands increases, however, it becomes more difficult to determine the underlying reasons for coordination site preferences and to separate electronic from steric effects. This is particularly true for multidentate organic ligands in which electronic and steric influences are often interconnected.

The bis(amino)cyclodiphosph(V)azanes *cis*-[(RHN)E=P(μ-N'Bu)₂P=E(NHR)] (R = 'Bu, Ar; E = O, S, Se, NR) (**A**, Chart 1) are well-known tetradentate molecules [3–5], whose coordination chemistry has only recently

been systematically investigated [6]. These ambidentate ligands chelate metal moieties as bis(amido) (*N,N'*) ligands above the heterocycle (**B**) [7] as bis(chalcogenido) (*E,E'*) ligands below the heterocycles (**C**) [8], or as a combination of both, namely as bis(amido)/bis(chalcogenido) ligands, i.e., *N,N'* and *E,E'* (**D**) [9,10]. The, thus far, most common coordination mode observed, however, is one in which the metal ions are coordinated laterally, similar to aminophosphoranes in either a monoanionic (*N,E*) (**E**) [11,12] or a dianionic (*N,E*)/(*N',E'*) (**F**) fashion [10,13]. A unique combination of facial and lateral coordination modes was reported by Chivers et al. [14,15] for the dilithio salt **G**. But most of these reactions were done with different cyclodiphosph(V)azanes, in different solvents, at different temperatures and with a variety of metallating agents, even for the same metal, thereby clouding the role of the ligand on the outcomes of these reactions.

We hoped to obtain insight into the role of the bis(amino)cyclodiphosph(V)azanes themselves on

* Corresponding author. Tel.: +(701)7772242; fax: +(701)7772331.
E-mail address: l.stahl@chem.und.edu (L. Stahl).

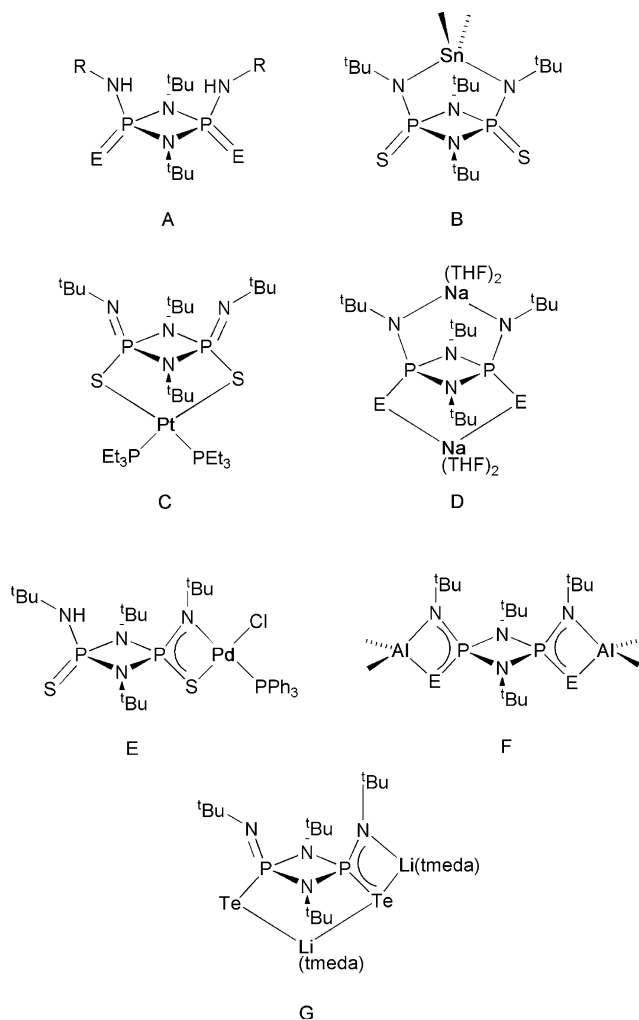


Chart 1.

product distribution and product structure by doing these reactions with the same organometallic reagent while systematically varying the ligand. Diethylzinc seemed a good choice as a metallating agent because it had been used successfully in reactions with related ligands [16,17]. It was also hoped that its relatively low reactivity would discriminate between the acidities of different ligands and between different coordination sites in the same ligand. In addition, zinc is of intermediate size, thereby preventing the structural bias introduced by very large or very small ions.

2. Experimental

2.1. General procedures

All experiments were performed under an atmosphere of purified nitrogen or argon, using standard Schlenk techniques. Solvents were dried and freed of molecular oxygen by distillation under an atmosphere of nitrogen

from sodium–benzophenone–ketyl or potassium–benzophenone–ketyl immediately before use. NMR spectra were recorded on a Bruker AVANCE-500 NMR spectrometer. The ^1H , ^{13}C and ^{31}P NMR spectra are referenced relative to $\text{C}_6\text{D}_5\text{H}$ (7.15 ppm), C_6D_6 (128.0 ppm) and $\text{P}(\text{OEt})_3$ (137.0 ppm), respectively. Melting points were obtained on a Mel-Temp apparatus and are uncorrected. Elemental analyses were performed by E and R Microanalytical Services, Parsippany, New Jersey, and Desert Analytics, Tucson, Arizona.

Diethylzinc was purchased from Acros and used as a 0.91 M hexanes stock solution. The cyclodiphosphazanes *cis*-[CIP(μ -N t Bu) $_2$ PCl][18], *cis*-[(t BuHN)P(μ -N t Bu) $_2$ P(NH t Bu)] [19,20] and *cis*-[(t BuHN)E=P(μ -N t Bu) $_2$ P=E(NH t Bu)], E = O [13], S [3], Se [9] were prepared by previously published procedures.

2.2. Syntheses

2.2.1. $\{[(\text{O}=\text{PN}^t\text{Bu})_2(\text{N}^t\text{Bu})_2\text{ZnEt}](\text{ZnEt}\cdot\text{THF})\}_2$ (1)

To a two-necked round-bottomed flask equipped with an addition funnel, inlet, and stir bar, was added **7** (0.792 g, 2.08 mmol). This was dissolved in THF (20 mL) and toluene (15 mL), and the ensuing solution was cooled to -78°C . To the vigorously stirring solution, ZnEt_2 (5.71 mL, 5.20 mmol) in THF (10 mL) was added slowly over 30 min. Once addition was complete, the solution was allowed to warm to RT and left to react for 24 h. The solution was then concentrated in vacuo and placed in a freezer at -21°C . After 16 h, 1.09 g (82.2%) of colorless crystals was isolated.

Mp: 203°C dec. ^1H NMR (500.13 MHz, benzene- d_6 , 26°C) δ = 3.57 (s, 8H, THF), 1.68 (br s, 9H, N t Bu), 1.65 (br s, 9H, N t Bu), 1.52 (s, 24H, N t Bu and CH_3 (Et)), 1.49 (m, 6H, CH_3), 1.41 (s, 8H, THF), 1.33 (s, 18H, N t Bu), 1.23 (s, 18H, N t Bu), 0.49 (m, 4H, CH_2), 0.35 (m, 4H, CH_2). $^{13}\text{C}\{^1\text{H}\}$ NMR (125.76 MHz, benzene- d_6 , 26°C) δ = 67.77 (s, THF), 55.32 (m, N t Bu), 52.97 (m, N t Bu), 33.31 (s, N t Bu), 32.02 (m, N t Bu), 31.04 (m, N t Bu), 25.76 (s, THF), 20.41 (s, CH_3), 12.69 (d, $J_{\text{PC}} = 10.51$ Hz, CH_3), 3.89 (s, CH_2), 0.70 (s, CH_2). $^{31}\text{P}\{^1\text{H}\}$ NMR (202.46 MHz benzene- d_6 , 26°C) δ = 5.66 (d, $J_{\text{PP}} = 42.58$ Hz), -3.24 (d, $J_{\text{PP}} = 39.01$ Hz). Anal. Calcd. for $\text{C}_{48}\text{H}_{108}\text{N}_8\text{O}_6\text{P}_4\text{Zn}_4$: C, 45.08; H, 8.51; N, 8.76. Found: C, 45.03; H, 8.54; N, 8.90%.

2.2.2. $\{[(^t\text{BuHN})\text{S}=\text{P}(\mu\text{-N}^t\text{Bu})_2\text{P}=\text{S}(\text{N}^t\text{Bu})](\text{ZnEt}\cdot\text{THF})\}_2$ (2)

A cold (-78°C) toluene/THF solution of [(t BuHN)S=P(μ -N t Bu) $_2$ P=S(NH t Bu)] (0.650 g, 1.58 mmol) was treated dropwise with ZnEt_2 (3.40 mL, 3.10 mmol). The reaction mixture was allowed to warm to room temperature, stirred at that temperature for 16 h and then concentrated to 5 mL in vacuo. After the flask had been stored at -21°C for several days, colorless crystals separated. Yield: 0.496 g (54.3%).

Mp: 71 °C dec. ^1H NMR (500.13 MHz, benzene- d_6 , 26 °C) δ = 3.57 (t, 4H, THF), 2.87 (s, 1H, HN t Bu), 1.65 (s, 18H, N t Bu), 1.48 (t, 3H, CH $_3$, J_{HH} = 8.1 Hz), 1.34 (t, 4H, THF), 1.33 (s, 9H, N t Bu), 1.21 (s, 9H, N t Bu), 0.78 (q, 2H, CH $_2$, J_{HH} = 8.1 Hz). $^{13}\text{C}\{^1\text{H}\}$ NMR (125.76 MHz, benzene- d_6 , 26 °C) δ = 68.07 (s, THF), 57.63 (s, N t Bu), 55.66 (d, J_{PC} = 13.8 Hz, N t Bu), 54.82 (s, N t Bu), 33.26 (d, J_{PC} = 9.9 Hz, N t Bu), 31.65 (d, J_{PC} = 4.2 Hz, N t Bu), 30.53 (t, J_{PC} = 4.5 Hz, N t Bu), 25.93 (s, THF), 12.60 (s, CH $_3$), 1.77 (s, CH $_2$). $^{31}\text{P}\{^1\text{H}\}$ NMR (202.46 MHz, benzene- d_6 , 26 °C) δ = 36.84 (d, J_{PP} = 23.4 Hz), 31.85 (d, J_{PP} = 25.2 Hz). Anal. Calcd. for C $_{22}$ H $_{50}$ N $_4$ OP $_2$ S $_2$ Zn: C, 45.71; H, 8.72; N, 9.69. Found: C, 45.37; H, 9.10; N, 10.04%.

2.2.3. $\{[(^t\text{BuHN})\text{Se}=\text{P}(\mu\text{-N}^t\text{Bu})_2\text{P}=\text{Se}(\text{N}^t\text{Bu})](\text{ZnEt}\cdot\text{THF})\}$ (3)

In a manner identical to that used for the synthesis of 2, $[(^t\text{BuHN})\text{Se}=\text{P}(\mu\text{-N}^t\text{Bu})_2\text{P}=\text{Se}(\text{N}^t\text{Bu})]$ (0.528 g, 1.04 mmol) was allowed to react with ZnEt $_2$ (2.85 mL, 2.60 mmol). Yield: 0.675 g (96.6%).

Mp: 66–69 °C. ^1H NMR (500.13 MHz, benzene- d_6 , 26 °C) δ = 3.57 (t, 4H, THF), 3.14 (s, 1H, HN t Bu), 1.69 (s, 18H, N t Bu), 1.50 (t, 3H, CH $_3$, J_{HH} = 8.1 Hz), 1.42 (t, 4H, THF), 1.34 (s, 9H, N t Bu), 1.20 (s, 9H, N t Bu), 0.81 (q, 2H, CH $_2$, J_{HH} = 8.1 Hz). $^{13}\text{C}\{^1\text{H}\}$ NMR (125.76 MHz, benzene- d_6 , 26 °C) δ = 68.04 (s, N t Bu), 58.39 (s, N t Bu), 56.86 (d, J_{PC} = 17.1 Hz, N t Bu), 55.49 (s, N t Bu), 33.07 (d, J_{PC} = 10.3 Hz, N t Bu), 31.67 (d, J_{PC} = 3.9 Hz, N t Bu), 30.62 (t, J_{PC} = 4.3 Hz, N t Bu), 25.94 (s, THF), 12.67 (s, CH $_3$), 2.91 (s, CH $_2$). $^{31}\text{P}\{^1\text{H}\}$ NMR (202.46 MHz, benzene- d_6 , 26 °C) δ = 22.45 (d, J_{PP} = 14.3 Hz), 11.88 (d, J_{PP} = 14.1 Hz). Anal. Calcd. for C $_{22}$ H $_{50}$ N $_4$ OP $_2$ Se $_2$ Zn: C, 39.33; H, 7.50; N, 8.34. Found: C, 38.99; H, 7.59; N, 8.28%.

2.2.4. $\text{cis-}[\text{ClP}(\mu\text{-N}^t\text{Bu})_2\text{P}(\text{NH}^t\text{Bu})]$ (4)

This is a simplified version of a previously published synthesis. To a cold (–78 °C) solution of phosphorus trichloride (200 mmol) and triethylamine (300 mmol) in 200 mL of hexanes was added dropwise *tert*-butylamine (500 mmol). A thick, white precipitate of triethylammonium chloride formed almost immediately. The reaction mixture was allowed to warm and stirred at RT for 12 h. It was then filtered on a large, coarse frit and the clear, colorless filtrate was concentrated in vacuo and stored at –12 °C until colorless needles had formed. Yield: 20.9 g (67.0%)

Mp: 70–74 °C. ^1H NMR (500.13 MHz, benzene- d_6 , 25 °C): δ = 3.78 (br s, 1 H), 1.34 (s, 18 H), 1.05 (s, 9 H). $^{13}\text{C}\{^1\text{H}\}$ NMR (125.76 MHz, benzene- d_6 , 25 °C): δ = 53.1 (t, J_{PC} = 8.4 Hz), 52.1 (d, J_{PC} = 7.3 Hz), 32.6 (d, J_{PC} = 4.9 Hz), 31.1 (t, J_{PC} = 6.5 Hz). $^{31}\text{P}\{^1\text{H}\}$ NMR (202.46 MHz, benzene- d_6 , 25 °C): δ = 194.6 (d, P–Cl, J_{PP} = 21.0 Hz), 135.8 (d, P–NH t Bu, J_{PP} = 20.8 Hz).

2.2.5. $\text{cis-}[(\text{PhHN})\text{S}=\text{P}(\mu\text{-N}^t\text{Bu})_2\text{P}=\text{S}(\text{NH}^t\text{Bu})]$ (5)

Aniline (1.16 mL, 12.7 mmol), dissolved in 60 mL toluene and cooled to 0°, was treated dropwise with *n*-BuLi (5.10 mL, 12.7 mmol). The resulting solution was heated to reflux for 1 h, allowed to cool to RT, and treated with a solution of 4 (3.61 g, 11.6 mmol) in 30 mL of toluene. The reaction-mixture was allowed to stir for 16 h at RT and filtered through a medium-porosity frit to remove lithium chloride. Elemental sulfur (0.743 g, 23.2 mmol) was then added, and the solution was kept at 50 °C for 4 h. The solution was then concentrated in vacuo to a volume of 20 mL and kept at –21 °C, until several fractions of off-white crystals had yielded 3.39 g (67.7%) of product.

Mp: 165 °C dec. ^1H NMR (500.13 MHz, benzene- d_6 , 26 °C) δ = 6.98 (t, 2H, J_{HP} = 7.7 Hz, *o*-Ph), 6.90 (d, 2H, J_{HP} = 7.5 Hz, *m*-Ph), 6.82 (t, 1H, J_{HP} = 7.4 Hz, *p*-Ph), 5.06 (d, J_{HP} = 13.2 Hz, 1H, HNPh), 3.00 (s, 1H, HN t Bu), 1.61 (s, 18H, N t Bu), 1.25 (s, 9H, N t Bu). $^{13}\text{C}\{^1\text{H}\}$ NMR (125.76 MHz, benzene- d_6 , 26 °C) δ = 140.54 (s, *i*-Ph), 129.41 (s, *o*-Ph), 128.31 (s, *m*-Ph), 121.95 (d, J_{PC} = 5.0 Hz, *p*-Ph), 57.04 (s, N t Bu), 54.46 (s, N t Bu), 31.32 (d, J_{PC} = 15.9 Hz, N t Bu), 29.66 (t, J_{PC} = 4.4 Hz). $^{31}\text{P}\{^1\text{H}\}$ NMR (202.46 MHz, benzene- d_6 , 26 °C) δ = 38.77 (d, J_{PP} = 34.1 Hz), 37.6 (br d). Anal. Calcd. For C $_{18}$ H $_{34}$ N $_4$ P $_2$ S $_2$: C, 49.97; H, 7.92; N, 12.97. Found: C, 49.94; H, 7.98; N, 13.22%.

2.2.6. $\{[(^t\text{BuHN})\text{S}=\text{P}(\mu\text{-N}^t\text{Bu})_2\text{P}=\text{S}(\text{NPh})]_2\text{Zn}\}$ (6)

A cold (–78 °C) toluene/THF solution of 5 (0.446 g, 1.03 mmol) was treated dropwise with ZnEt $_2$ (2.07 mL, 1.88 mmol), dissolved in a toluene/THF solvent mixture. Once the addition was complete, the reaction mixture was allowed to warm to room temperature and stirred for 14 h. The solution was then concentrated in vacuo and placed in a freezer at –78 °C. Several crops of colorless crystals yielded 0.456 g (95.3%) of product.

Mp: 280–282 °C. ^1H NMR (500.13 MHz, benzene- d_6 , 26 °C) δ = 7.44 (d, 4H, J_{HP} = 8.0 Hz, *o*-Ph), 7.13 (d, J_{HP} = 7.6 Hz, 4H, *m*-Ph), 6.92 (t, J_{HP} = 6.8 Hz, 2H, *p*-Ph), 3.27 (s, 2H, HN t Bu), 1.58 (s, 36H, N t Bu), 1.29 (s, 18H, N t Bu). $^{13}\text{C}\{^1\text{H}\}$ NMR (125.76 MHz, benzene- d_6 , 26 °C) δ = 147.81 (d, J_{PC} = 12.5 Hz, *i*-Ph), 129.87 (s, *o*-Ph), 128.70 (s, *m*-Ph), 123.04 (d, J_{PC} = 13.8 Hz, *p*-Ph), 57.27 (d, J_{PC} = 3.8 Hz, N t Bu), 54.71 (s, N t Bu), 31.33 (d, J_{PC} = 4.0 Hz, N t Bu), 29.99 (t, J_{PC} = 4.1 Hz, N t Bu). $^{31}\text{P}\{^1\text{H}\}$ NMR (202.46 MHz, benzene- d_6 , 26 °C) δ = 38.31 (d, J_{PP} = 25.2 Hz), 37.69 (d, J_{PP} = 25.3 Hz). Anal. Calcd. for C $_{36}$ H $_{66}$ N $_8$ P $_4$ S $_4$ Zn: C, 46.57; H, 7.16; N, 12.07. Found: C, 46.59; H, 7.27; N, 11.78%.

2.2.7. $[(^t\text{BuNH})\text{S}=\text{P}(\mu\text{-N}^t\text{Bu})_2\text{P}=\text{Np-tolyl}(\text{NH}^t\text{Bu})]$ (7)

A sample of $[(^t\text{BuNH})\text{P}(\mu\text{-N}^t\text{Bu})_2\text{P}(\text{NH}^t\text{Bu})]$ (4.99 g, 14.3 mmol), dissolved in 80 mL of toluene, was treated at room temperature with a toluene solution (10 mL) of

p-tolyl azide (1.91 g, 14.3 mmol). After the reaction mixture had been stirred for 16 h, it was treated with sulfur (0.459 g, 14.3 mmol) and allowed to react at room temperature for an additional 3 h. The solution was concentrated to 40 mL in vacuo and stored in a freezer (−21 °C) for several days. Yield: 5.57 g (80.1%).

Mp: 163–165 °C. ¹H NMR (500.13 MHz, benzene-d₆, 26 °C) δ = 7.63 (d, *J*_{HH} = 7.9 Hz, 2 H, *p*-tolyl), 7.19 (d, *J*_{HH} = 7.6 Hz, 2H, *p*-tolyl), 2.65 (d, *J*_{HP} = 5.6 Hz, 1H, HN^{*t*}Bu), 2.22 (s, 3H, Me-*p*-tolyl), 1.93 (br s, 1H, HN^{*t*}Bu), 1.51 (s, 18H, N^{*t*}Bu), 1.42 (s, 9H, N^{*t*}Bu), 1.21 (s, 9H, N^{*t*}Bu). ¹³C{¹H} NMR (125.76 MHz, benzene-d₆, 26 °C) δ = 145.69 (s, ipso-*p*-tolyl), 129.86 (d, *J*_{PC} = 1.3 Hz, *o*-*p*-tolyl), 128.70 (s, *m*-*p*-tolyl), 125.10 (d, *J*_{PC} = 21.9 Hz, *p*-*p*-tolyl), 55.9 (s, N^{*t*}Bu), 54.2 (t, *J*_{PC} = 4.3 Hz, N^{*t*}Bu), 32.06 (d, *J*_{PC} = 4.6 Hz, N^{*t*}Bu), 31.61 (d, *J*_{PC} = 4.3 Hz, N^{*t*}Bu), 30.79 (t, *J*_{PC} = 4.1 Hz, N^{*t*}Bu), 21.09 (s, Me-*p*-tolyl). ³¹P{¹H} NMR (202.46 MHz, benzene-d₆, 26 °C) δ = 35.48 (d, *J*_{PP} = 39.7 Hz), −23.22 (d, *J*_{PP} = 40.1 Hz). Anal. Calcd. for C₂₃H₄₅N₅P₂S: C, 56.89; H, 9.34; N, 14.42. Found: C, 57.08; H, 9.58; N, 14.43%.

2.2.8. $\{[(^t\text{BuHN})\text{S}=\text{P}(\mu\text{-N}^t\text{Bu})_2\text{P}=\text{Np-tolyl}(\text{N}^t\text{Bu})](\text{ZnEt})\}$ (**8**)

In a manner identical to those used for the syntheses of **2** and **3**, a toluene/THF solution of **7** (0.484 g, 0.997 mmol) was treated with ZnEt₂ (2.73 mL, 2.49 mmol). Yield: 0.548 g (96.1%) of colorless crystals.

Mp: 115–120 °C. ¹H NMR (500.13 MHz, benzene-d₆, 26 °C) δ = 7.68 (d, *J*_{HH} = 8.2 Hz, 2 H, *tolyl*), 7.21 (d, *J*_{HH} = 8.2 Hz, 2H, *tolyl*), 2.98 (s, 1H, HN^{*t*}Bu), 2.22 (s, 3H, Me-*tolyl*), 1.61 (t, *J*_{HH} = 8.1 Hz, 3H, Me), 1.44 (s, 18H, N^{*t*}Bu), 1.37 (s, 9H, N^{*t*}Bu), 1.30 (s, 9H, N^{*t*}Bu), 0.88 (q, *J*_{HH} = 8.1 Hz, CH₂). ¹³C{¹H} NMR (125.76 MHz, benzene-d₆, 26 °C) δ = 143.85 (s, ipso-Ph), 129.58 (s, *o*-Ph), 128.24 (s, *m*-Ph), 121.63 (d, *J*_{PC} = 16.2 Hz, *p*-Ph), 56.15 (s, N^{*t*}Bu), 54.01 (s, N^{*t*}Bu), 51.02 (s, N^{*t*}Bu), 33.77 (d, *J*_{PC} = 8.3 Hz, N^{*t*}Bu), 31.34 (d, *J*_{PC} = 4.1 Hz, N^{*t*}Bu), 30.55 (t, *J*_{PC} = 4.1 Hz, N^{*t*}Bu), 20.58 (s, Me-*tolyl*), 12.47 (s, CH₂), 1.16 (s, Me). ³¹P{¹H} NMR (202.46 MHz, benzene-d₆, 26 °C) δ = 35.89 (d, *J*_{PP} = 36.5 Hz), 1.12 (d, *J*_{PP} = 34.0 Hz). Anal. Calcd. for C₂₅H₄₉N₅P₂SZn: C, 51.85; H, 8.53; N, 12.10. Found: C, 51.87; H, 8.86; N, 12.06%.

2.3. X-ray crystallography

2.3.1. Compounds **1**, **4**, **5** and **8**

Suitable, single crystals were coated with oil, affixed to a glass capillary, and centered on the diffractometer. Reflection intensities were collected with a Bruker SMART CCD diffractometer, equipped with an LT-2 low-temperature apparatus. Intensity data for compounds **1** and **5** were collected at room temperature, while those of **4** and **8** were collected at −60 °C. Data

were measured using ω scans of 0.3° per frame for 30 s until a complete hemisphere had been collected. The first 50 frames were recollected at the end of the data collection to monitor for decay. The crystals of **1** decomposed at room temperature and cracked at low temperature. It was therefore necessary to rapidly collect its intensity data at room temperature using ω scans of 3.0° per frame for 30 s with a final resolution of 0.80 e/Å³. This data acquisition mode leads to lower precision in the derived structure parameters.

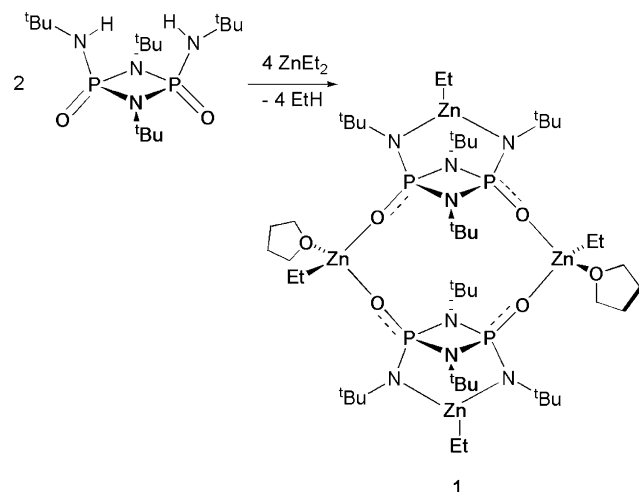
Cell parameters were retrieved using SMART [21] software and refined with SAINT [22] on all observed reflections. Data were reduced with SAINT, which corrects for Lorentz and polarization effects and decay. An empirical absorption correction was applied with SADABS [23]. The structures were solved by direct methods with the SHELXS 90 [24] program and refined by full-matrix least squares methods on *F*² with SHELXL 97 [25], incorporated in SHELXTL Version 5.10 [26].

2.3.2. Compounds **2**, **3** and **7**·1.5(THF)

The crystals were obtained as indicated in Section 2. Compound **7** did not give suitable single crystals in the absence of THF, but single crystals could be obtained when the colorless powder was recrystallized from THF. In compound **7**·1.5(THF) the inversion center at 1/2, 0, 1/2 is occupied by one-half molecule of THF. This disordered molecule was modeled using 0.5 oxygen atoms and two methylene groups, i.e.; O_{0.5}C₂H₄. This model leads to two orientations of the THF molecule which are related to each other by inversion symmetry. Because the data were collected at RT and because of the low electron-densities at these positions, we did not attempt to split the methylene carbon atoms. The final difference map showed no electron density greater, or less, than about 0.32 e/Å³. The crystals were sealed inside argon-filled glass capillaries, and the intensity data were collected at room temperature on a Bruker P4 diffractometer. The structures were solved by direct-methods with SHELXL NT, Version 5.10, and were refined analogously to **1**, **4**, **5** and **8**.

3. Results

In order to ensure that the product distribution was not affected by solubility, all reactions were done in THF-toluene solvent mixtures, in which both reactants and products were very soluble. We began our reactivity studies with the deprotonation of the di(*tert*-butylamino)-dioxo-substituted heterocycle *cis*-[(^{*t*}BuHN)O=P(μ-N^{*t*}Bu)₂P=O(NH^{*t*}Bu)], whose bis(dimethylaluminum) derivative had shown bilateral coordination (**F**, Chart 1). On addition of two equivalents of diethylzinc to this ligand we obtained (Scheme 1), again, a bimetallic complex, namely $\{[(\text{O}=\text{PN}^t\text{Bu})_2(\text{N}^t\text{Bu})_2\text{ZnEt}](\text{ZnEt} \cdot$



Scheme 1.

(THF)₂ (**1**). Composition and NMR spectra, however, suggested that it was not as symmetrical as the dialuminum species. For example, two mutually coupled doublets in the ³¹P NMR spectrum indicated two non-identical phosphorus environments. A single-crystal X-ray analysis proved that **1** had indeed an entirely different structure than the aluminum analogue. Selected data collection and bond parameters of this complex are given in Tables 1 and 2, respectively.

As Fig. 1 shows, this complex consists of two monoethylzinc bis(amido)cyclodiphosph(V)azanes, which are connected to a centrosymmetric dimer by bridging ethylzinc moieties. A potentially higher symmetry is prevented by the displacement of both cyclod-

Table 2
Bond lengths (Å) and angles (°) of **1**

Bond lengths	
Zn(1)–C(17)	1.981(7)
Zn(1)–O(1)	1.980(4)
Zn(1)–O(2)	1.981(4)
Zn(1)–O(3)	2.193(4)
Zn(2)–C(23)	2.014(9)
Zn(2)–N(3)	2.028(4)
Zn(2)–N(4)	2.047(4)
P(1)–N(3)	1.592(5)
P(2)–N(4)	1.598(5)
P(1)–N(1)	1.669(4)
P(1)–N(2)	1.700(4)
P(2)–N(1)	1.679(4)
P(2)–N(2)	1.688(4)
P(1)–O(1)	1.495(4)
P(2)–O(2)	1.497(4)
Bond angles	
O(1)–Zn(1)–O(2)	107.08(15)
O(1)–Zn(1)–O(3)	96.88(17)
O(2)–Zn(1)–O(3)	92.95(17)
C(17)–Zn(1)–O(1)	112.7(3)
C(17)–Zn(1)–O(2)	130.6(3)
C(17)–Zn(1)–O(3)	109.7(2)
N(3)–Zn(2)–N(4)	109.20(13)
C(23)–Zn(2)–N(4)	122.7(3)
C(23)–Zn(2)–N(3)	128.1(3)
N(1)–P(1)–N(2)	83.06(19)
N(1)–P(2)–N(2)	83.1(2)
P(1)–O(1)–Zn(1)	160.4(2)
P(2)–O(2)–Zn(1)	150.8(2)

iphosphazanes with respect to each other by the repulsive interactions of their *tert*-butylimino groups. The two chemically distinct ethylzinc moieties display

Table 1
Crystal and refinement data for compounds **1–5**, **7** · 1.5(THF) and **8**

	1	2	3	4	5	7 · 1.5(THF)	8
Chemical formula	C ₄₈ H ₁₀₈ N ₈ O ₆	C ₂₂ H ₅₀ N ₄ OP ₂	C ₂₂ H ₅₀ N ₄ OP ₂	C ₁₂ H ₂₇ ClN ₃ P ₂	C ₁₂ H ₂₈ ClN ₃ P ₂	C ₂₉ H ₅₇ N ₅ O _{1.5}	C ₂₅ H ₄₉ N ₅ P ₂ S
Fw	1278.91	578.09	671.93	311.76	432.55	593.80	579.06
Space group	<i>P</i> 2 ₁ / <i>n</i> (No. 14)	<i>P</i> 2 ₁ 2 ₁ 2 ₁ (No. 19)	<i>P</i> 2 ₁ 2 ₁ 2 ₁ (No. 19)	<i>P</i> 2 ₁ (No. 4)	<i>P</i> 2 ₁ / <i>c</i> (No. 14)	<i>P</i> 2 ₁ / <i>n</i> (No. 14)	<i>P</i> $\bar{1}$ (No. 2)
<i>T</i> (°C)	23	23	22	–60	20	22	–60
<i>a</i> (Å)	9.921(6)	10.2675(8)	10.311(2)	9.6036(5)	16.8512(7)	9.5857(14)	9.4251(4)
<i>b</i> (Å)	18.202(11)	10.3381(13)	10.3956(17)	10.8116(6)	9.9622(4)	32.361(3)	10.3103(5)
<i>c</i> (Å)	18.141(11)	30.149(6)	30.398(10)	9.6355(5)	14.6847(6)	11.6507(10)	16.3432(8)
α (°)							95.4570(10)
β (°)	90.782(7)			115.678(1)	103.9850(10)	102.176(9)	100.7820(10)
γ (°)							97.1370(10)
<i>V</i> (Å ³)	3276(3)	3200.2(8)	3258.5(13)	901.65(8)	2392.12(17)	3532.8(7)	1536.58(12)
<i>Z</i>	2	4	4	2	4	4	2
ρ_{calc} (g cm ^{–3})	1.297	1.200	1.707	1.145	1.201	1.116	1.252
λ (Å)	0.710 73	0.710 73	0.710 73	0.710 73	0.710 73	0.710 73	0.710 73
μ (cm ^{–1})	15.91	10.17	38.38	3.80	3.66	2.11	9.93
<i>R</i> (<i>F</i>) ^a [<i>I</i> > σ (<i>I</i>)]	0.0556	0.0343	0.0624	0.0518	0.0353	0.0477	0.0313
<i>wR</i> 2(<i>F</i> ²) ^b (all data)	0.1088	0.0999	0.1746	0.1252	0.1088	0.1432	0.0838

$$w = 1/[\sigma^2(F_o)^2 + (xP)^2 + yP], \text{ where } P = (F_o^2 + 2F_c^2)/3.$$

$$^a R = \sigma|F_o - F_c|/\sigma|F_o|.$$

$$^b R_w = \{[\sigma w F_o^2 - F_c]^2 / [w \Sigma F_o^2]\}^{1/2}.$$

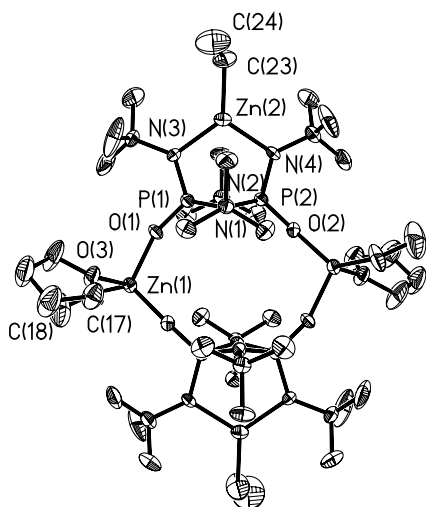


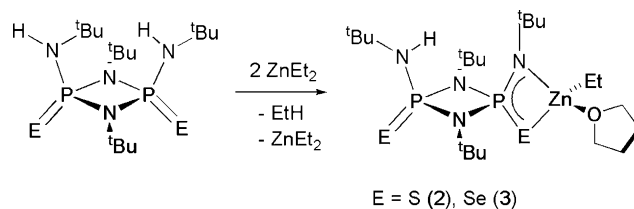
Fig. 1. Thermal-ellipsoid (35% probability) plot and partial numbering scheme of **1**. Hydrogen atoms have been omitted for clarity.

different coordination environments; one zinc atom is *N,N'*-chelated by the bis(amido) substituents above the (PN)₂ ring, as in **B**, while the second zinc atom is coordinated by a THF molecule and two phosphoryl oxygen atoms from different ligands.

The chelation of an ethylzinc moiety by both amido groups is not unexpected, but the coordination by the phosphoryl oxygen atoms is unusual and, as far as we know, unprecedented for this ligand system. The three-coordinate zinc atom has a perfectly trigonal-planar coordination environment and forms two slightly asymmetrical Zn–N bonds (2.028(4) and 2.047(4) Å) that are only insignificantly longer than those of related amido-coordinated zinc ions [17,27,28]. The second zinc atom (Zn1) is in a distorted ZnO₃C environment. The zinc–oxygen bonds to the phosphoryl groups are equidistant (1.980(4) and 1.981(4) Å) and thus quite comparable in length to those with bridging isopropoxide groups (1.983(3) Å) [28]. The THF donor bond to zinc is expectedly longer (2.193(4) Å) and appears to be among the longest bonds of this type, which normally range from about 2.00 to 2.10 Å [29,30]. The zinc–carbon bonds (2.014(9) and 1.981(7) Å), by contrast, are similar in length to those of related complexes with three-coordinate zinc ions [17,31].

Given their partial-negative charge and di-coordination, the oxygen atoms form surprisingly short phosphorus–oxygen bonds (1.495(4) Å) that are not much longer than those in the pristine ligand (1.467(2) Å) [32]. As the result of the asymmetry in the dimer, the P–O–Zn bond angles are unequal, spanning 150.8(2)° and 160.4(2)°, respectively.

To determine if this unusual coordination behavior of the ligand was retained in the disulfur and diselenium analogues, we repeated this reaction with *cis*-[(^tBuHN)E=P(μ-^tN'Bu)₂P=E(NH'^tBu)], E = S, Se



Scheme 2.

(Scheme 2) under identical conditions. In both cases the bis(amino)cyclodiphosph(V)azanes reacted cleanly with only one of the two equivalents of diethylzinc added, producing the mono(ethylzinc) compounds $\{[(^t\text{BuHN})\text{E}=\text{P}(\mu\text{-N}'\text{Bu})_2\text{P}=\text{E}(\text{N}'\text{Bu})](\text{ZnEt}\cdot\text{THF})\}$, E = S (**2**), Se (**3**), respectively. Prolonged heating of these reaction mixtures revealed the presumed formation of symmetrically-coordinated bimetallic species having structures similar to **D** or **F**. These reactions were accompanied by considerable decomposition of the ligand and resulted in complex mixtures, and we, therefore, did not attempt to isolate these compounds. The diminished reactivity of **2** and **3** is likely due to their lesser acidity, sulfur and selenium being less electronegative than oxygen. The ³¹P NMR spectra of **2** and **3** exhibited two sets of mutually-coupled doublets, thereby confirming the lateral mono-coordination of each ligand by one ethylzinc moiety.

Single-crystal X-ray analyses on both complexes, whose crystal and data collection parameters are listed

Table 3
Selected bond lengths (Å) and angles (°) for **2** and **3**

	2	3
<i>Bond lengths</i>		
Zn–S(e)	2.4490(12)	2.5398(18)
Zn–N(3)	2.009(3)	2.020(7)
Zn–C(5)	1.962(5)	1.992(13)
Zn–O(1)	2.241(3)	2.236(8)
P(1)–S(e)(1)	2.0037(13)	2.154(2)
P(2)–S(e)(2)	1.9272(12)	2.077(2)
P(1)–N(3)	1.580(3)	1.581(8)
P(1)–N(1)	1.695(3)	1.692(7)
P(1)–N(2)	1.684(3)	1.697(7)
P(2)–N(1)	1.688(3)	1.678(7)
P(2)–N(2)	1.699(3)	1.685(8)
P(2)–N(4)	1.632(3)	1.602(10)
<i>Bond angles</i>		
S(e)–Zn–N(3)	78.22(9)	80.2(2)
N(3)–Zn–O(1)	104.60(14)	105.6(3)
O(1)–Zn–S(e)(1)	95.97(9)	95.8(2)
O(1)–Zn–C(5)	102.0(2)	101.8(5)
Zn(1)–S(e)(1)–P(1)	76.75(4)	73.39(7)
Zn(1)–N(3)–P(1)	101.18(15)	102.5(4)
N(3)–P(1)–S(e)(1)	103.85(12)	103.9(3)
N(1)–P(1)–N(2)	83.48(13)	82.3(3)
N(1)–P(2)–N(2)	83.52(14)	83.1(3)
N(4)–P(2)–S(e)(2)	112.66(120)	112.3(3)
P(1)–N(1)–P(2)	96.24(14)	97.1(3)
P(1)–N(2)–P(2)	95.83(14)	96.6(3)

in Table 1, confirmed this structure assignment. Table 3 provides a side-by-side comparison of selected bond parameters for these isostructural molecules, for which the solid-structure of **2** is shown representatively in Fig. 2. In these spirocyclic complexes one side of the ligand coordinates the zinc atom in a distorted tetrahedral fashion, the bond angles ranging from $78.22(9)^\circ$ to $105.6(3)^\circ$. While the zinc–nitrogen and zinc–oxygen bonds are identical in both compounds, the shorter ethyl–zinc bond of the sulfur analogue may reflect the lesser steric crowding in this compound. The Zn–S bond (2.4480(12) Å) is somewhat longer than that in $\{[\text{Me}_2\text{Si}(\mu\text{-N}^t\text{Bu})_2\text{P}=\text{S}(\text{NPh})_2\text{Zn}]\}$ [33], while the Zn–Se (2.5398(18) Å) bond is almost identical in length to that in a tetracoordinate zinc complex having two acyclic amino(seleno)phosphoranate ligands [27].

The comparatively small change on going from oxygen to the heavier chalcogens thus caused a rather large change in the outcomes of these reactions, supporting our contention that zinc is a good probe for electronic variations in bis(amino)cyclodiphosph(V)azanes. We therefore decided to investigate the role of the organic amino-substituents on the outcomes of these reactions. It may be recalled that AlMe_3 reacted with all ligands, namely $[(\text{RHN})\text{E}=\text{P}(\mu\text{-N}^t\text{Bu})_2\text{P}=\text{E}(\text{NHR})]$, $\text{E} = \text{O}, \text{S}, \text{Se}$; $\text{R} = ^t\text{Bu}, \text{Ph}$, under double-deprotonation with the formation of analogous bimetallic products [13].

Upon changing the amino-substituent from *tert*-butyl to phenyl we discovered that the phenyl-substituted diamine $[(\text{PhHN})\text{S}=\text{P}(\mu\text{-N}^t\text{Bu})_2\text{P}=\text{S}(\text{NHPh})]$ reacted with one equivalent of diethylzinc to form off-white powders, whose insolubility made a structural analysis impossible [34]. Although not conclusive, the insolubility suggests the formation of a dianionic ligand, involved in bilateral metal chelation. Because of the contrasting behavior – *tert*-butyl-substituted ligands form monomers while phenyl-substituted ligands form oligomers or polymers – it was of interest to synthesize a ligand bearing both, a *tert*-butylamino and an anilino group.

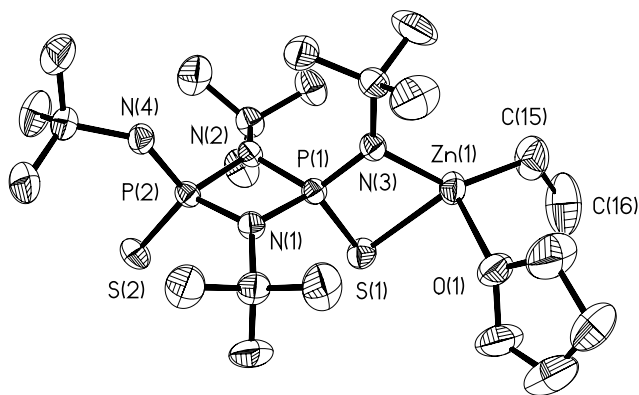


Fig. 2. Thermal-ellipsoid (35% probability) plot and partial numbering scheme of **2**. Compound **3** is isostructural. Hydrogen atoms have been omitted for clarity.

Such asymmetrically-substituted species are readily accessible from the monochlorocyclodiphosph(III)azane *cis*- $[\text{ClP}(\mu\text{-N}^t\text{Bu})_2\text{P}(\text{NH}^t\text{Bu})]$ (**4**) [35]. This known compound was synthesized by a simplified method, and its solid-state structure is presented in Fig. 3. Crystal data and selected bond parameters of **4** are listed in Tables 1 and 4, respectively.

The monochlorocyclodiphosph(III)azane is a $\text{P}(\mu\text{-N}^t\text{Bu})_2\text{P}$ heterocycle, bearing two almost coplanar *tert*-butyl groups and two *cis*-configured exocyclic phosphorus substituents. The exocyclic phosphorus substituents (chloro and *tert*-butylamino) form obtuse angles with the heterocycle. As is commonly observed for these molecules, the lone exocyclic P–N bond is shorter (1.659(3) Å) than the endocyclic ones, but the latter are decidedly unequal, the bonds to the chlorine-bearing phosphorus atom being much shorter (1.665(3) vs. 1.744(3) Å). Donation of the nitrogen lone-pair into the σ^* orbital of the P–Cl bond has lengthened this bond (2.2047(13) Å) substantially beyond the sum of covalent radii of P and Cl (2.09 Å) [36]. This bond is also

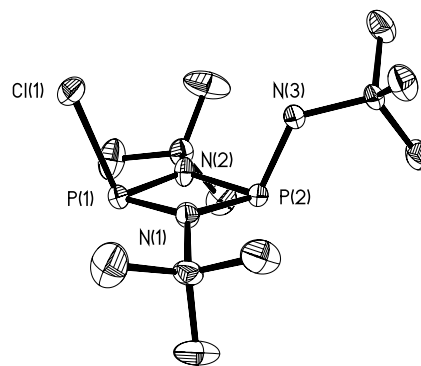


Fig. 3. Thermal-ellipsoid (35% probability) plot and partial numbering scheme of **4**. Hydrogen atoms have been omitted for clarity.

Table 4
Selected bond lengths (Å) and angles ($^\circ$) for **4** and **5**

	4	5
<i>Bond lengths</i>		
P(1)–Cl(1), N(3)	2.2047(13)	1.6480(15)
P(2)–N(3), N(4)	1.659(3)	1.6289(15)
P(1)–N(1)	1.680(3)	1.6743(15)
P(1)–N(2)	1.665(3)	1.6767(15)
P(2)–N(1)	1.752(3)	1.7042(14)
P(2)–N(2)	1.744(3)	1.6902(15)
P(1)–S(1)	–	1.9317(6)
P(2)–S(2)	–	1.9247(6)
<i>Bond angles</i>		
N(1)–P(1)–N(2)	83.34(14)	84.23(7)
N(1)–P(2)–N(2)	79.11(13)	82.91(7)
N(3)–P(1)–S(1)	–	108.80(6)
N(4)–P(2)–S(2)	–	113.69(6)
P(1)–N(1)–P(2)	98.1(2)	95.84(7)
P(1)–N(2)–P(2)	98.9(2)	96.28(8)

significantly longer than the P–Cl bonds (2.105(9) Å) in the dichloro analogue, *cis*-[ClP(μ-N^tBu)₂PCl], of this molecule [37].

When **4** was treated with one equivalent of lithium anilide (Scheme 3), the asymmetrically-substituted cyclodiphosph(III)azane *cis*-[(^tBuHN)P(μ-N^tBu)₂P(NHPh)] was obtained, which upon oxidation with sulfur furnished the cyclodiphosph(V)azane *cis*-[(^tBuHN)S=P(μ-N^tBu)₂P=S(NHPh)] (**5**); its solid-state structure is shown in Fig. 4. This molecule is a hybrid of *cis*-[(^tBuHN)S=P(μ-N^tBu)₂P=S(NH^tBu)] [4] and *cis*-[(PhHN)S=P(μ-N^tBu)₂P=S(NHPh)] [13], whose structures are known. Crystal and data collection parameters for **5** are listed in Table 1, while selected bond lengths and angles are given in Table 4.

It is a common structural feature of bis(amino)dithiocyclodiphosph(V)azanes that one amino substituent has an *endo* conformation, while the second one retains its conventional *exo* conformation. Compound **5** is no exception, and it comes as no surprise that the smaller phenyl substituent occupies the more crowded *endo* position. The asymmetry of **5** is much less pronounced than that of **4**, as reflected in smaller differences of similar bonds. Thus, the P–N(H)^tBu bond is shorter (1.6289(15) Å) than the P–N(H)Ph bond (1.6480(15) Å), while the endocyclic P–N bonds of the *tert*-butyl-

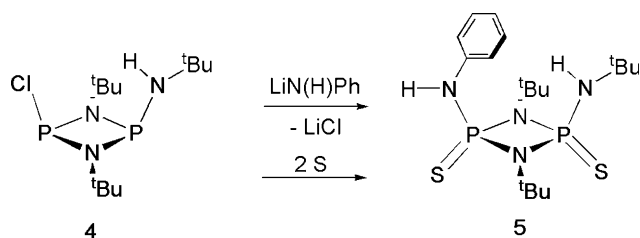
substituted phosphorus atom are longer (avg. 1.6972(15) Å vs. 1.6755(15) Å).

This molecule was allowed to react with two equivalents of diethylzinc with the intention of obtaining a dizinc species (Scheme 4), containing metal ions in different chemical environments. The ¹H NMR data, however, showed that the product had the opposite composition, i.e., it was a monozinc–diligand complex, namely, {[(^tBuHN)S=P(μ-N^tBu)₂P=S(NHPh)]₂Zn} (**6**). An analogous product was obtained by Chivers et al. [6] when they treated [(^tBuHN)Se=P(μ-N^tBu)₂P=Se(NH^tBu)] with one equivalent of ZnMe₂.

The outcome of this reaction thus demonstrates the much greater reactivity of the anilino- versus the *tert*-butylamino-substituted side of the ligand. Because we recently reported the X-ray structure analysis of the related {[Me₂Si(μ-N^tBu)₂P=S(NHPh)]₂Zn} [33], which shows a tetrahedral zinc atom chelated by two P=S(NHPh) moieties, it may be assumed that **6** is a similar trispirocycle. The structure of **6** is an indication that the product of the reaction between [(PhHN)S=P(μ-N^tBu)₂P=S(NHPh)] and diethylzinc is, indeed, an oligomer or a polymer.

Competitive reactions such as this clearly show the different reactivities of dissimilar coordination sites in bis(amino)cyclodiphosph(V)azanes and demonstrate the importance of the amino substituents on the outcomes of the reactions. Thus, by merely substituting one side of the cyclodiphosphazane with a *tert*-butyl group, the degree of metallation can be controlled and condensation prevented.

Ligand asymmetry can also be introduced by the addition of two nonidentical chalcogens or by mixed (chalcogen/imino) groups on phosphorus. Such asymmetrically-substituted cyclodiphosph(V)azanes can be obtained even more easily than those discussed above, by oxidizing cyclodiphosph(III)azanes sequentially with two different reagents, as shown in Scheme 5. Thus, the sequential treatment of [(^tBuHN)P(μ-N^tBu)₂P(NH^tBu)] with one equivalent of *p*-tolyl azide and one equivalent of elemental sulfur afforded the asymmetrically



Scheme 3.

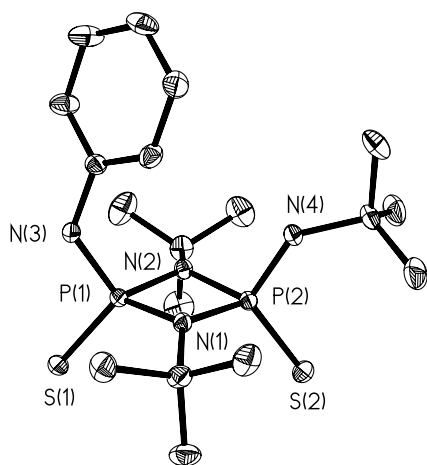
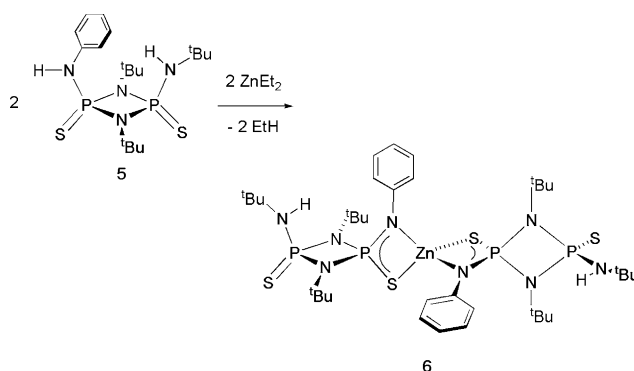
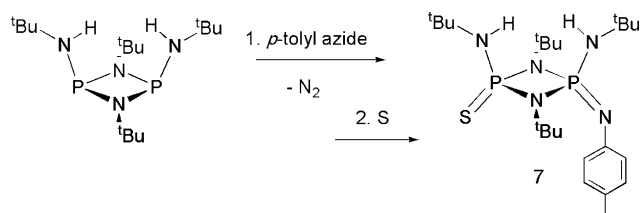


Fig. 4. Thermal-ellipsoid (35% probability) plot and partial numbering scheme of **5**. Hydrogen atoms have been omitted for clarity.



Scheme 4.



Scheme 5.

P-substituted [(^tBuNH)S=P(μ-^tBu)₂P=N*p*-tol(NH^t-Bu)] (**7**). Single crystals, suitable for X-ray analysis, could only be obtained as a sesqui-tetrahydrofuranate of **7**, namely **7** · 1.5(THF).

The solid-state structure of this cyclodiphosph(V)azane in **7** · 1.5(THF) is shown in Fig. 5, while crystal and selected bond parameters are listed in Tables 1 and 5, respectively. In contrast to the bis(amino)cyclodiphosph(V)azane dichalcogenides, here both *tert*-butyl substituents of the amino nitrogens are in an *exo* position, and the *p*-tolylimino group is coplanar with the N2–P2–N1 moiety, suggestive of conjugation effects. The molecule has three distinctly different P–N bonds, namely four equidistant, endocyclic P–N bonds (avg. 1.689(2) Å), two equidistant exocyclic P–N(H)^tBu bonds (avg. 1.634(2) Å) and one unique phosphorus–tolylimino bond (1.542(2) Å). These phosphorus–nitrogen bonds, as well as the lone phosphorus–sulfur bond (1.9334(9) Å), have lengths similar to those found in related bis(amino)cyclodiphosph(V)azanes [4,13].

Because this ligand bears identical *tert*-butylamino groups, its acidity and coordinative selectivity now rests solely on the second exocyclic phosphorus substituents, namely *p*-tolylimino and sulfur. While the sulfur side of the ligand is sterically more accessible, π-electron-delocalization is more effective at the amino/imino side of the ligand, presumably making it more acidic. The treatment of **7** with two equivalents of diethylzinc (Scheme 6) yielded again only a monometallic, monoligand complex, similar to **2** and **3**.

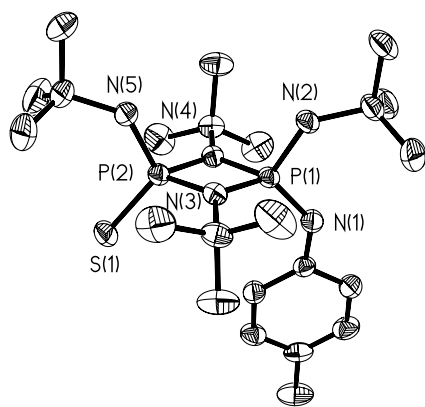
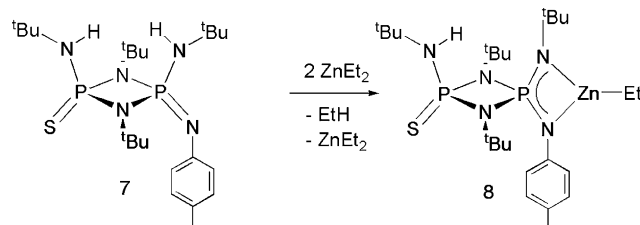


Fig. 5. Thermal-ellipsoid (35% probability) plot and partial numbering scheme of **7**. Hydrogen atoms have been omitted for clarity.

Table 5
Selected bond lengths (Å) and angles (°) for **7** · 1.5(THF) and **8**

	7 · 1.5(THF)	8
<i>Bond lengths</i>		
Zn(1)–C(1)	–	1.946(2)
Zn(1)–N(1)	–	2.0077(16)
Zn(1)–N(2)	–	1.9954(15)
P(1)–N(1)	1.5391(19)	1.6080(15)
P(1)–N(2)	1.6316(18)	1.5934(15)
P(1)–N(3)	1.6889(18)	1.6834(15)
P(1)–N(4)	1.6895(18)	1.6885(15)
P(2)–N(3)	1.6845(19)	1.7000(15)
P(2)–N(4)	1.6816(18)	1.6909(15)
P(2)–N(5)	1.633(2)	1.6350(16)
P(2)–S(1)	1.9334(8)	1.9247(7)
<i>Bond angles</i>		
N(1)–Zn(1)–N(2)	–	73.83(6)
N(1)–Zn(1)–C(1)	–	139.15(8)
N(2)–Zn(1)–C(1)	–	146.53(8)
N(1)–P(1)–N(2)	106.58(10)	97.36(8)
N(3)–P(1)–N(4)	82.91(9)	83.33(7)
P(1)–N(3)–P(2)	96.82(9)	96.83(8)
P(1)–N(4)–P(2)	96.90(9)	96.99(8)
N(3)–P(2)–N(4)	83.28(9)	82.76(7)
N(5)–P(2)–S(1)	118.98(8)	116.64(6)



Scheme 6.

Both amino protons can be distinguished by ¹H NMR spectroscopy, and it was therefore evident that the *N,N'*, rather than the *N,S* side, had reacted and chelated the zinc atom. These solution NMR findings were confirmed by a single crystal X-ray analysis of **8**, whose data collection and selected bond parameters are collected in Tables 1 and 5, respectively. The ORTEP diagram (Fig. 6) shows that compound **8** is a spirocycle of two four-membered rings, one being terminated by a trigonal-planar zinc atom. The ligand coordinates the zinc atom as an almost perfectly-symmetrical amino(imino)phosphoranate. Thus, in notable contrast to the distinctly different phosphorus–nitrogen bonds in the pristine ligand (P1–N1 = 1.540(2) Å and P1–N2 = 1.633(2) Å), these bonds have almost identical lengths (avg. 1.6007(15) Å), as do the Zn–N1 and Zn–N2 bonds (avg. 2.0016(16) Å). These latter bonds are slightly shorter than those of the three-coordinate zinc atom in **1**, possibly reflecting the superiority of the lateral coordination of these ligands.

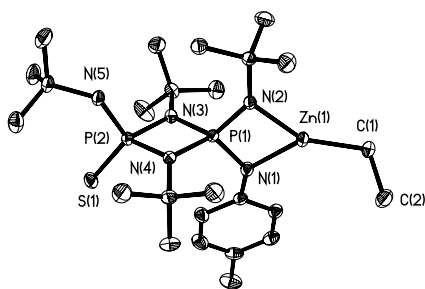


Fig. 6. Thermal-ellipsoid (35% probability) plot and partial numbering scheme of **8**. Hydrogen atoms have been omitted for clarity.

4. Discussion

Despite their comparatively recent dates, studies on the coordination chemistry of bis(amino)cyclodiphosph(V)azanes have revealed clear trends [6], regarding both the degree of deprotonation and the coordination sites of these molecules. With the present study we have tried to add to our understanding of coordinative preferences of these ligands by focusing on ligand-substituent effects.

Bis(amino)cyclodiphosph(V)azanes have four exocyclic phosphorus substituents (R_1 , R_2 , E_1 and E_2) which can be altered independently of each other (Chart 2) leading to a large variety of possible molecules. To keep the number of ligands and their complexes manageable we chose two primary amines, namely, *tert*-butylamine and aniline, and four oxidants, namely organic peroxides, sulfur, selenium and *p*-tolyl azide. With these reasonably diverse ligands we hoped to shed some light on the inherent acidities and coordination preferences of bis(amido)cyclodiphosph(V)azanes.

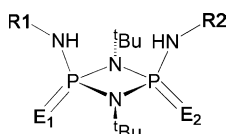


Chart 2.

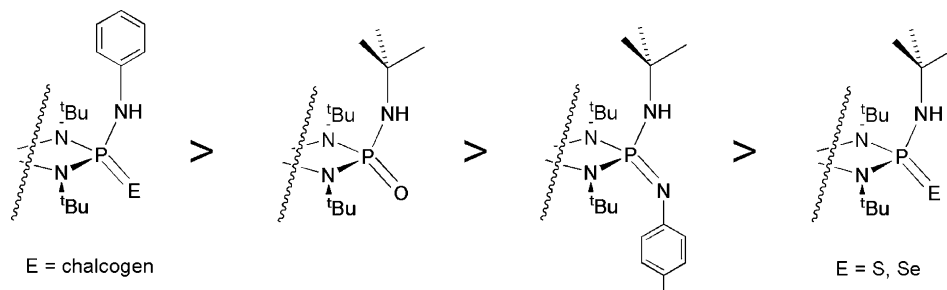


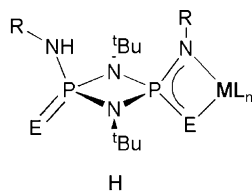
Chart 3.

The degree of deprotonation of bis(amino)cyclodiphosph(V)azanes – and this is no surprise – depends both on the reactivities of the metallating agents and the acidity of the bis(amino)cyclodiphosph(V)azanes themselves. Thus, with all bis(amino)cyclodiphosph(V)azanes the more polar and thus more reactive group 1- and group 13-metal alkyls form bimetallic species. A similar leveling effect is seen with the most acidic ligands, and bis(anilino)cyclodiphosph(V)azanes invariably form dianionic species, no matter what metallating agent is used [6,12,13].

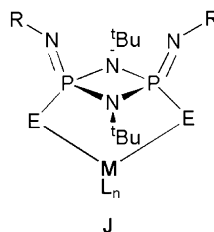
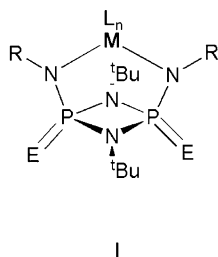
The less reactive diethylzinc, however, does discriminate between the acidities of the various bis(amino)cyclodiphosph(V)azanes. Diethylzinc, for example, dimetallates only the most acidic bis(*tert*-butylamino)cyclodiphosph(V)azane, namely, *cis*-[*t*-BuHN]O=P(μ -N'*t*-Bu)₂P=O(NH'*t*-Bu)] cleanly, while the sulfur and selenium analogues react reluctantly with a second equivalent of base. The relative reactivities of the various bis(amino)cyclodiphosph(V)azanes are summarized in Chart 3, and they can be interpreted entirely in terms of the Brønsted acidities of these ligands.

Equally predictable as the degree of deprotonation is the coordination site preference of mono-anionic ligands. In general, and in keeping with results from other investigators [6,10,11], monoanionic ligands coordinate metals laterally (Chart 4, Case 1, **H**), and this can be understood in terms of the π -electron delocalization over the *N,P,E* or *N,P,N'* moieties at the sides of the ligands. For these monoanionic ligands the coordination site preference follows the acidities of the various sites shown in Chart 3, thus ligand sides having anilino groups are preferred over those having *tert*-butylamino groups, and *N,N'* coordination is preferred over *N,S* and *N,Se* coordination. The *N,N'* sites apparently also donate more electron density to the zinc moieties, because zinc ions are three-coordinate when chelated by two nitrogen atoms, but four-coordinate when chelated by *N,S* and *N,Se* groups, with THF occupying the fourth coordination site.

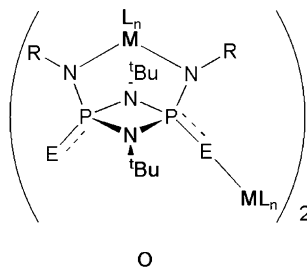
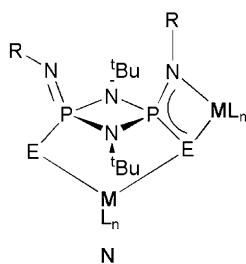
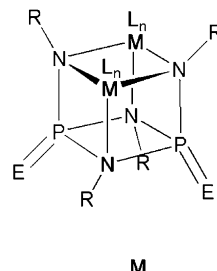
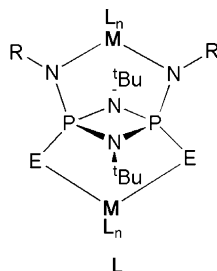
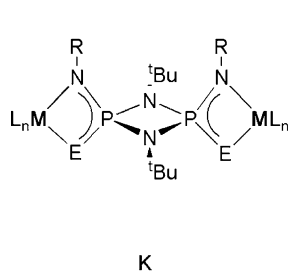
Monometallic complexes of dianionic ligands exhibit only one of two coordination modes, with the lone metal chelated above (Case 2, **I**) or below the (PN)₂ ring (**J**).



Case 1: mono-anionic-monometallic species



Case 2: di-anionic-monometallic species



Case 3: di-anionic-bimetallic species

Chart 4.

Only one example for each of these modes has been confirmed, with the respective binding site presumably being dictated by HSAB considerations. Thus, tin(IV) and platinum(II) were chelated by both amido or both sulfur atoms, respectively.

Dianionic bis(amido)cyclodiphosph(V)azanes bearing two metal moieties offer the greatest potential for structural variety, and this is borne out by the diversity of the isolated compounds. Five different coordination modes have been authenticated by X-ray crystallography thus far, and these are shown schematically as Case 3 in Chart 4. The by far most common coordination mode is the bilateral one (**K**), with the bifacial (**L**) and

the heterocubic (**M**) modes being the next most common. Based on the data from previous studies by Chivers [6,9–11], Scherer [39] and Nöth [7], it appears that bis(amido)cyclodiphosph(V)azanes coordinate two metals laterally (**K**) as long as the covalent radius of the metal is less than about 1.28 Å. Thus aluminum has shown exclusively lateral coordination, but metal atoms with larger covalent radii (Na, K) prefer the sterically more accessible positions above and below the (PN)₂ ring (**L**). The coordination modes **N** and **O** are hybrids of facial- and lateral-coordinations, and each has been observed only once thus far. Highly sterically-encumbered metal moieties, i.e., metals bearing additional

ligands, seem to prefer the more open lateral coordination sites (**K**) because of excessive steric crowding above the (PN)₂ ring, while **M** has only been observed in cases where the ligand was formed in situ [38,39].

5. Supporting information available

Crystallographic data for the structural analyses have been deposited with the Cambridge Crystallographic Data Centre, CCDC, Nos. 221020–221026 for compounds **1–5**, **7** · 1.5(THF) and **8**, respectively. Copies of this information may be obtained free of charge from: The Director, CCDC, 12 Union Road, Cambridge CB2 EZ UK (Fax: +44-1223-336033); deposit@ccdc.cam.ac.uk or [www.http://ccdc.cam.ac.uk](http://ccdc.cam.ac.uk).

Acknowledgements

We thank the Chevron Phillips Chemical Company for financial support of this research and the National Science Foundation for a GAANN fellowship (to GRL).

References

- [1] A.H. Norbury, A.I.P. Sinha, *Q. Rev.* 5 (1970) 69.
- [2] J.L. Burmeister, *Coord. Chem. Rev.* 3 (1968) 225.
- [3] C.-C. Chang, R.C. Haltiwanger, M.L. Thompson, H.-W. Chen, A.D. Norman, *Inorg. Chem.* 18 (1979) 1899.
- [4] T.G. Hill, R.C. Haltiwanger, M.L. Thompson, S.A. Katz, A.D. Norman, *Inorg. Chem.* 33 (1994) 1770.
- [5] M.D. Noiro, E.G. Bent, A.D. Norman, *Phosphorus Sulfur* 62 (1991) 177.
- [6] For a comprehensive review, see: G.G. Briand, T. Chivers, M. Krahn, *Coord. Chem. Rev.* 233–234 (2002) 237.
- [7] G. Linti, H. Nöth, E. Schneider, W. Storch, *Chem. Ber.* 126 (1993) 619.
- [8] T. Chivers, C. Fedorchuk, M. Krahn, M. Parvez, G. Schatte, *Inorg. Chem.* 40 (2001) 1936.
- [9] T. Chivers, M. Krahn, M. Parvez, *Chem. Commun.* (2000) 463.
- [10] T. Chivers, M. Krahn, M. Parvez, G. Schatte, *Inorg. Chem.* 40 (2001) 2547.
- [11] G.G. Briand, T. Chivers, G. Schatte, *Inorg. Chem.* 41 (2002) 1958.
- [12] D.F. Moser, C.J. Carrow, L. Stahl, R.J. Staples, *J. Chem. Soc., Dalton Trans.* (2001) 1246.
- [13] G.R. Lief, C.J. Carrow, L. Stahl, R.J. Staples, *Organometallics* 20 (2001) 1629.
- [14] G.G. Briand, T. Chivers, M. Parvez, *Angew. Chem., Int. Ed. Engl.* 41 (2002) 3468.
- [15] G.G. Briand, T. Chivers, M. Parvez, G. Schatte, *Inorg. Chem.* 42 (2003) 525.
- [16] G.T. Lawson, C. Jacob, A. Steiner, *Eur. J. Inorg. Chem.* (1999) 1881.
- [17] S.K. Pandey, A. Steiner, H.W. Roesky, D. Stalke, *Inorg. Chem.* 32 (1993) 5444.
- [18] O.J. Scherer, P. Klusmann, *Angew. Chem., Int. Ed. Engl.* 8 (1969) 752.
- [19] I. Schranz, L. Stahl, R.J. Staples, *Inorg. Chem.* 37 (1998) 1493.
- [20] R.R. Holmes, J.A. Forstner, *Inorg. Chem.* 2 (1963) 380.
- [21] SMART V 4.043 Software for the CCD Detector System, Bruker Analytical X-ray Systems, Madison, WI, 1995.
- [22] SAINT V 4.035 Software for the CCD Detector System, Bruker Analytical X-ray Systems, Madison, WI, 1995.
- [23] SADABS program for absorption corrections using the Bruker CCD Detector System. Based on: R. Blessing, *Acta Crystallogr. A* 51 (1995) 33.
- [24] G.M. Sheldrick, SHELXS 90, Program for the Solution of Crystal Structures, University of Göttingen, Göttingen, Germany, 1990.
- [25] G.M. Sheldrick, SHELXL 97, Program for the Solution of Crystal Structures, University of Göttingen, Göttingen, Germany, 1997.
- [26] SHELXTL 5.10 (PC-Version), Siemens Analytical X-Ray Instruments, Inc. Madison, WI, 1998.
- [27] M. Bochmann, G.C. Bwembya, M.B. Hursthouse, S.J. Coles, *J. Chem. Soc., Dalton Trans.* (1995) 2813.
- [28] M. Cheng, A.B. Attygalle, E.B. Lobkovsky, G.W. Coates, *J. Am. Chem. Soc.* 121 (1999) 11583.
- [29] D.J. Darensbourg, M.W. Holtcamp, G.E. Struck, S.A.N. Zimmer, P. Rainey, J.B. Robertson, J.D. Draper, J.H. Reibenspies, *J. Am. Chem. Soc.* 121 (1999) 107.
- [30] C. Kimblin, B.M. Bridgewater, D.G. Churchill, G. Parkin, *Chem. Commun.* (1999) 2301.
- [31] J. Prust, A. Stasch, W. Zheng, H.W. Roesky, E. Alexopoulos, I. Usón, D. Böhler, T. Schuchardt, *Organometallics* 20 (2001) 3825.
- [32] G.R. Lief, D.C. Haagenson, R.J. Staples, L. Stahl, in preparation.
- [33] D.C. Haagenson, D.F. Moser, L. Stahl, R.J. Staples, *Inorg. Chem.* 41 (2002) 1245.
- [34] G.R. Lief, L. Stahl, unpublished results.
- [35] R. Jefferson, J.F. Nixon, T.M. Painter, R. Keat, L. Stobbs, *J. Chem. Soc., Dalton Trans.* (1973) 1414.
- [36] L. Pauling, *The Nature of the Chemical Bond*, third ed., Cornell University Press, Ithaca, 1960.
- [37] K.W.J. Muir, *J. Chem. Soc., Dalton Trans.* (1975) 259.
- [38] T. Chivers, M. Krahn, M. Parvez, G. Schatte, *Chem. Commun.* (2001) 2547.
- [39] O.J. Scherer, P. Quintus, J. Kaub, W.S. Sheldrick, *Chem. Ber.* (1987) 1183.